

This material may be downloaded for personal use only. Any other use requires prior permission of the American Society of Civil Engineers. This material may be found at <https://ascelibrary.org/doi/10.1061/9780784484982.037>.

1 Axial Cyclic Behavior of FRP Confined Seawater Sea-Sand Concrete Piles

2 Numan Malik;¹ Jian-Hua Yin;²
 3 Wen-Bo Chen;³ Wu Pei-chen;⁴
 4 Zejian Chen;⁵

5 ¹Ph.D. Candidate, Department of Civil and Environmental Engineering, The Hong Kong
 6 Polytechnic University, Email: numan.malik@connect.polyu.hk

7 ²Chair Professor, Department of Civil and Environmental Engineering, The Hong Kong
 8 Polytechnic University, Email: jian-hua.yin@polyu.edu.hk; cejhyin@polyu.edu.hk

9 ³Research Assistant Professor, Department of Civil and Environmental Engineering, The Hong
 10 Kong Polytechnic University, (Corresponding Author). Email: wb.chen@polyu.edu.hk

11 ⁴Research Assistant Professor, Department of Civil and Environmental Engineering, The Hong
 12 Kong Polytechnic University, Email: elvis.wu@polyu.edu.hk

13 ⁵Research Assistant Professor, Department of Civil and Environmental Engineering, The Hong
 14 Kong Polytechnic University, Email: zejchen@polyu.edu.hk

16 ABSTRACT

17 Fiber-reinforced polymer (FRP) composites coupled with seawater sea-sand concrete (SSC)
 18 provide an innovative and sustainable solution by replacing the conventional piling materials for
 19 the marine infrastructures. This study investigates the axial behavior of FRP composite SSC model
 20 piles subjected to cyclic loading of different amplitudes and mean loads levels. The strain along
 21 the depth of piles is measured by an advanced distributed optic sensing technique called optical
 22 frequency domain reflectometry (OFDR) having a spatial resolution of 1 mm and $\pm 1\mu\text{e}$ sensing
 23 accuracy. Three structural configurations; FRP tube confined and FRP rebars cage reinforced and
 24 centered FRP rebar SSC piles ended in rock-socket are investigated in physical models to examine
 25 the performance of FRP composites and SSC in pile foundations. The accumulated displacement
 26 of model piles under different modes of axial cyclic loading are analyzed and explored in detail. It
 27 is found that the accumulation of permanent cyclic displacement increases markedly initially till
 28 30 cycles and then followed a constant trend with increasing cycles passing. Under the same cyclic
 29 loading conditions, the FRP tube confined model piles exhibited lower cyclic degradation leading
 30 to stable behavior. The FRP tube confined model piles showed higher confinement and axial cyclic
 31 capacities compare to those reinforced with FRP rebars. The OFDR sensing technique monitored
 32 the localized effects efficiently that how the load is distributed along the length of model piles.

33 INTRODUCTION

34 The traditional pile foundations in a harsh marine environment experience severe corrosion of steel,
 35 marine borer attacks on the timber piles, and concrete deterioration causing many problems like
 36 failure of the structure and huge maintenance costs(Iskander & Hassan, 1998; Iskander & Stachula,
 37 2002). Apart, the consumption of large quantities of river sand and fresh water in the construction
 38 industry poses a major concern for future developments and environmental sustainability.
 39 However, steel reinforced concrete poses no compatibility due to chloride ions in sea water and
 40 sea sand which can enhance corrosion problems. Therefore fiber-reinforced polymer (FRP)
 41 composites coupled with seawater sea-sand concrete (SSC) provide an innovative and sustainable
 42 solution by replacing the conventional piling materials for the marine infrastructures.

43 Pile foundations are usually subjected to cyclic loadings caused by wind, water currents, waves,
44 earthquakes, traffic loads, and ice sheets. Cyclic loadings are variable and repeated in nature with
45 a different range of magnitudes and cycles (Jardine et al., 2013) The long-term axial cyclic
46 behavior of piles showed that the accumulated settlement of piles largely depends on the cycling
47 loading parameters (SharnoubiM.M. & NaggarM.H., 2012; Buckley et al., 2018). Although
48 numerous research work has been carried out on cyclic response of piles in sand, chalk, and soft
49 soils, the behavior of piles ended in rock-socket under cyclic loading is rarely reported. Apparently,
50 there is necessity of in-depth study of cyclic loading tests on piles in rock-socket, based on
51 systemic tests to provide guidance and potential predictive measures.

52 Traditionally, strain measurements for piles foundations are carried out by strain gauges and
53 vibrating wire extensometers which provide strain values at certain points resulting in less reliable
54 strain profile (De Battista et al., 2016). However, distributed fiber optic sensors (DFOS) have
55 overcome the strain measurement limitations providing continuous information along the whole
56 length of fiber. Many researchers have applied typical Brillouin optical time-domain reflectometry
57 (BOTDR) based DFOS having less spatial resolution in geotechnical applications such as
58 monitoring piles, tunnels, pipelines, natural slopes, retaining walls, and dams (Soga, 2014; Zhang
59 et al., 2015). A novel sensing technique with highest spatial resolution and accuracy called optical
60 frequency domain reflectometry (OFDR) has been adopted in this study. The OFDR sensing
61 technique was used to monitor the geogrid deformations of a laboratory model slope with smart
62 geogrids under various loadings (Sun et al., 2020). Similarly the load transfer curves and localized
63 strain variations of a continuous flight auger (CFA) pile were monitored by OFDR optic fibers
64 (Bersan et al., 2018).

65 This study examines the cyclic behavior of FRP-SSC composite model piles ended in rock socket
66 using a novel distributed sensing technology named OFDR possessing a higher spatial resolution
67 of 1mm and high sensing accuracy of $\pm 1\mu\epsilon$. The physical model piles were subjected to cyclic
68 loadings of different mean loads and amplitudes to investigate the accumulation and degradation
69 of permanent cyclic displacement with cycles. For future design and risk assessment
70 considerations, the results of this study will assist the geotechnical engineers.

71 **EXPERIMENTAL PROGRAM**

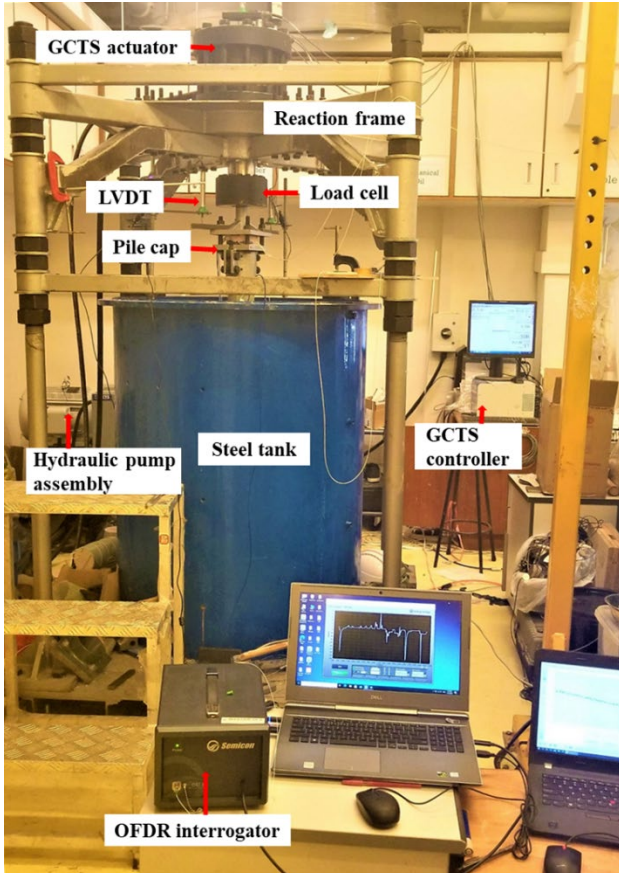
72 **Setup and Design of Physical Model piles**

73 For this study a physical model was designed consisting of hydraulic loading actuator (GCTS,
74 USA) that can apply both static and cyclic loads axially on pile head as shown in Figure 1(a).
75 Model piles were constructed in the steel tank having drilled rock with socket depth of 150 mm
76 and 100 mm diameter. The length to diameter ratio of rock socket was kept 1.5, falling within the
77 range of common geotechnical engineering practices (Ng et al., 2001).

78 A total of four model piles with different structural configurations, 1450 mm in length and 100
79 mm in diameter were modelled and tested in this study. Pile 1 and Pile 2 were confined with 3.5
80 mm thick GFRP tube, Pile 3 was reinforced with 9.5 mm diameter rebars, and Pile 4 has a centered
81 rebar of diameter 19 mm as shown in Figure 1(b). The GFRP tube serve as a formwork for first
82 two model piles and SSC was cast in it while for third pile the rebar cage was first fabricated and
83 then fixed in the socket followed by casting concrete inside.

84 The model piles were instrumented with an advanced distributed optical fiber sensing (DOFS)
85 system to measure the deformation along the pile depth based on Rayleigh backscattering through
86 OFDR sensing technique. The OFDR interrogator used in this study have a spatial resolution of 1
87 mm with measuring accuracy of ± 1.0 microstrain. Four OFDR sensing fibers were installed
88 longitudinally on GFRP tube for Pile 1 and Pile 2 with two fibers embedded in the SSC shown in
89 Figure 1(c). For Pile 3, fibers were installed on the rebars and within the SSC, as shown in Figure
90 1(c).

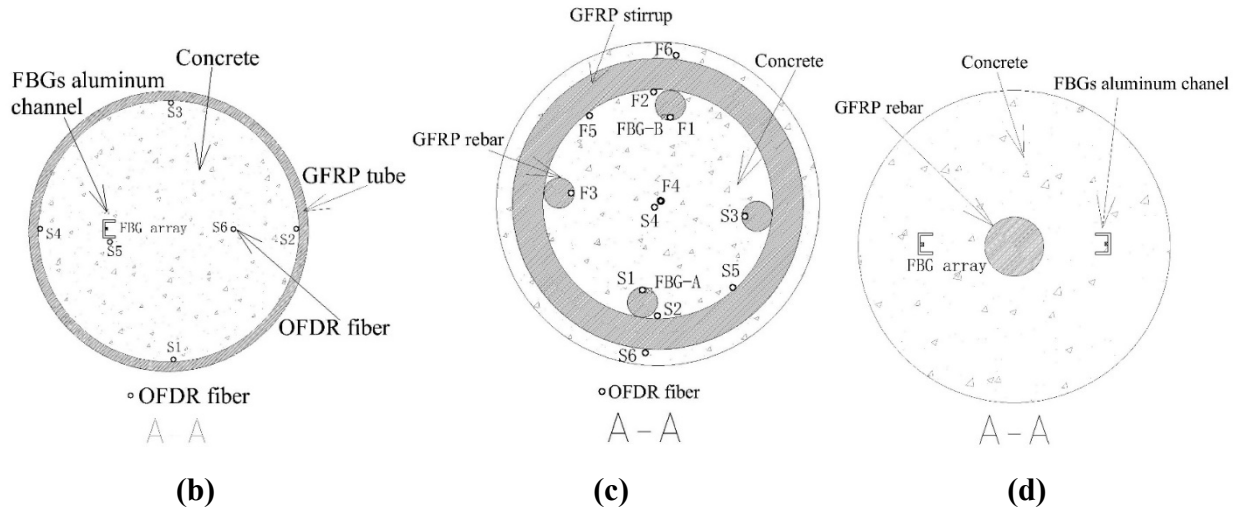
91 In addition, multiplexed FBGs were also instrumented, due to high data acquisition frequency for
92 cyclic loads.



93

94

(a)



95 **Figure 1. Physical model system: (a) setup of the whole physical model system; (b) Pile 1 or**
 96 **Pile 2; (c) Pile 3 ; and (d) Pile 4**

98 **TESTING PROGRAM**

99 The model piles were subjected to a series of cyclic loadings with different cyclic amplitudes and
 100 mean loads, summarized in Table. 4. Generally, offshore pile foundations experience cyclic loads
 101 with frequencies ranging between 0.0001 to 0.1 Hz and cycles from 10 to 10^5 (Puech, 2013). The
 102 frequency adopted in this study was 0.01 Hz with 100 cycles for each loading case. The model
 103 piles were unloaded after each stage of cyclic loading and then subjected to axial monotonic
 104 compression under the load control condition till the failure.

105 **Table 1.** Cyclic loading program of the model piles

Test pile	*Test Code	Mean Load Q_{mean} (kN)	Cyclic amplitude Q_{cyc} (kN)	Cycles applied N	Post cyclic compression capacity Q_{us} (kN)	Sinusoidal frequency (Hz)
Pile 1	P1.CY1	60	30	100	210	0.01
	P1.CY2	120	30	100		
	P1.CY3	120	45	50		
	P1.CY4	180	30	7		
Pile 2	P2.CY1	60	30	100	266	0.01
	P2.CY2	120	30			
	P2.CY3	120	45			
	P2.CY4	180	30			
Pile 3	P3.CY1	60	30	100	213	0.01
	P3.CY2	120	30			
	P3.CY3	120	45			
Pile 4	P4.CY1	60	30	100	239	0.2

106 *Test code (PX.CYN), where PX represents pile name (P1, P2, P3, P4) and CYN shows number
107 of cyclic test (N=1, 2, 3, 4).

108 **RESULTS AND DISCUSSIONS**

110 **Cyclic Parameters and Criteria**

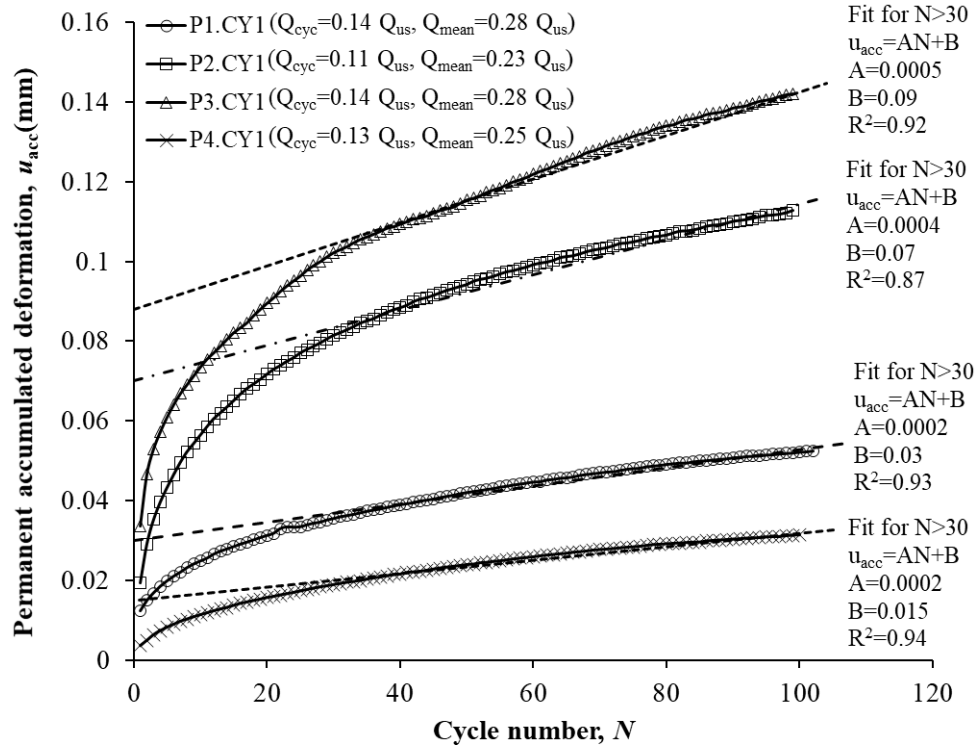
111 Under cyclic axial loading conditions, the behavior of piles driven in sand, clays, and chalk has
112 been classified as stable, meta stable, or unstable based on a specific stability criterion (Jardine &
113 Standing, 2012; Tsuha et al., 2012; Buckley et al., 2018). P1.CY4 was considered unstable,
114 P1.CY1, P2.CY1, P3.CY1 and P4.CY1 have stable response while the remaining eight cyclic
115 stages were appeared to have metastable behavior. The post-cycle monotonic static compression
116 capacity of the corresponding model piles was used to normalize the cyclic loading characteristics.

117 **Permanent accumulated cyclic displacement of model piles**

118 The accumulated cyclic displacement “ u_{acc} ” was calculated based on the formulations provided in
119 the study (Rimoy et al., 2013). For the cyclic tests on each model pile, the accumulation of pile-
120 head permanent cyclic displacement, u_{acc} , was plotted against the number of cycles, N . A constant
121 gradient fitting line is plotted for the cyclic tests for comparing accumulation having a linear trend
122 given as:

$$u_{acc} = AN + B \quad (1)$$

123 where A and B are non-dimensional fitting parameters. It was observed that in the cyclic stable
124 tests (Figure 2), stable and low accumulation of the displacements were recorded with a non-linear
125 gradient for the first 20 cycles. After $N > 30$, the rate of accumulated displacement follows the
126 constant gradient fitting line with negligible deviation from it afterward. Initially for $N < 20$, the
127 accumulation rate was as high as 0.02mm/cycle and then followed a steady rate of 0.01mm/20
128 cycles for $N > 30$. In the metastable tests (Figures 3 and 4), initially the rate of permanent
129 displacement accumulation was higher for $N < 30$, and afterward, it followed a constant gradient
130 fitting line of 0.03 mm/20 cycles. However, P2.CY2 and P2.CY3 metastable cyclic tests showed
131 a slow rate of permanent displacement accumulation comparatively. A metastable cyclic test,
132 P2.CY4, as shown in Figure 5, initially led to a very sharp rate of permanent accumulated
133 displacement for the first 10 cycles. The accumulation non-linearly increased till 40 cycles and
134 then followed a constant gradient fitting line for $N > 40$ with the rate of 0.034 mm/ 20 cycles.
135 During the unstable cyclic test P1.CY4 the displacement accumulation rate was sharp led to failure
136 of the model pile in 7 cycles.

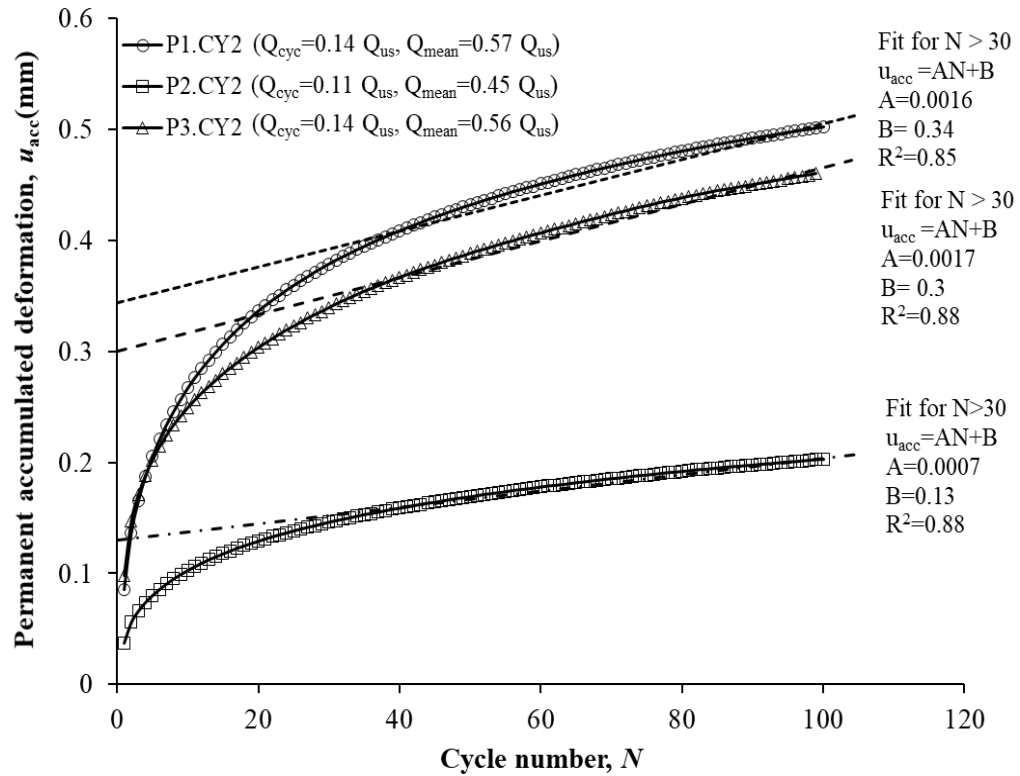


137

138

139

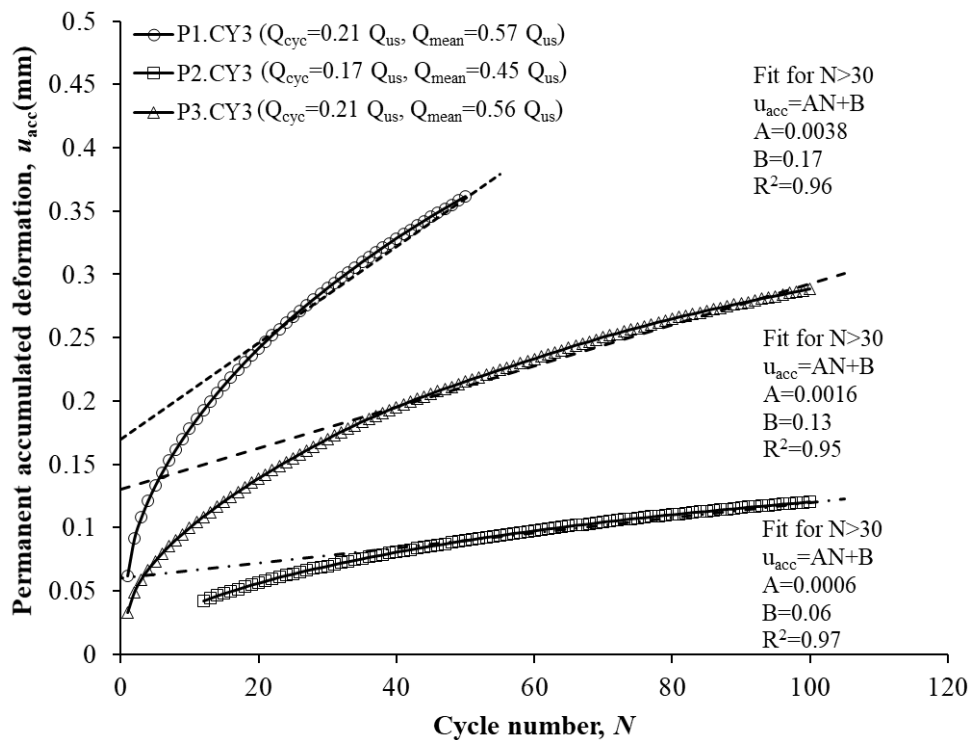
Figure 2. Accumulation of permanent cyclic displacement behavior for stable cyclic tests



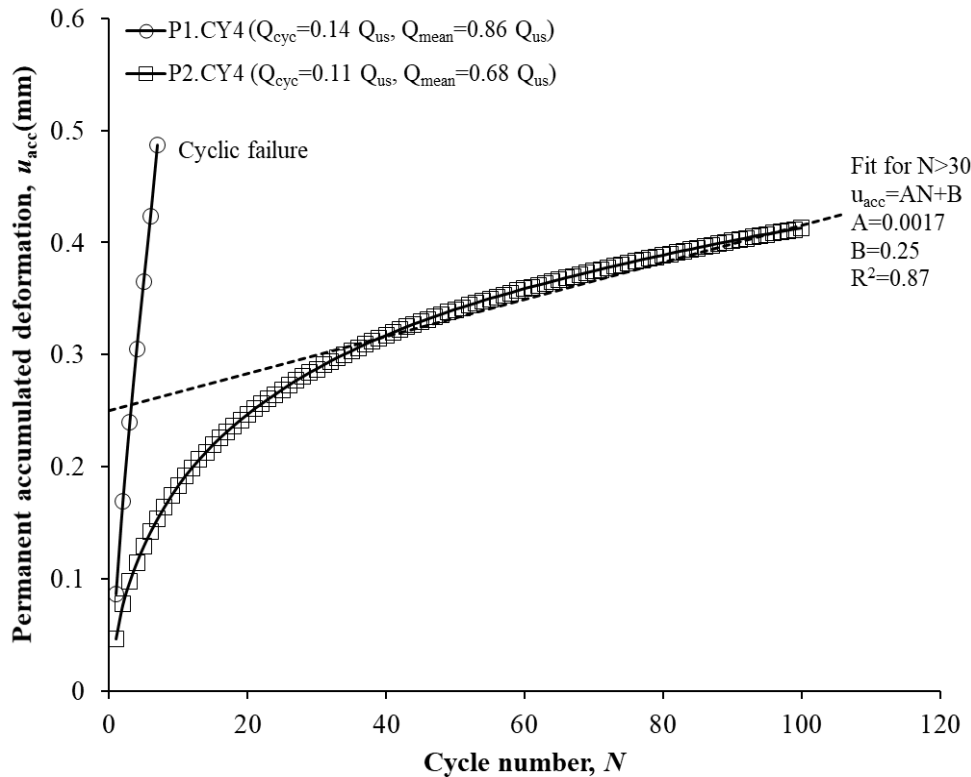
140

141

142 **Figure 3. Accumulation of permanent cyclic displacement behavior for metastable cyclic**
143 **tests**



144
145
146 **Figure 4. Accumulation of permanent cyclic displacement behavior for metastable cyclic**
147 **tests with higher Q_{cyc}**



148

149

150 **Figure 5. Accumulation of permanent cyclic displacement behavior for unstable/metastable**
151 **cyclic tests**

152 **CONCLUSION**

153 Pile foundations must be durable, economical, and long-lasting in order to guarantee the structural
154 integrity of infrastructures. This study describes a series of axial cyclic loading tests performed on
155 FRP composite SSC physical model piles in rock-socket under varying cyclic amplitudes and mean
156 loads. For monitoring the accumulation of permanent cyclic displacement of the physical model
157 piles, OFDR and FBG sensing technologies were used. It was found that the permanent cyclic
158 displacement responses of model piles are influenced by normalized cyclic loading levels. For
159 stable, metastable, and unstable tests, the load-displacement behavior is highly nonlinear in the
160 first 20, 30, and 40 cycles, respectively. For $N > 30$, cyclic displacement accumulation was
161 significant in the initial cycles and then followed a constant gradient trendline for subsequent
162 cycles, which can be incorporated in numerical models to predict the behavior of the same type of
163 piles. Further in-depth study is required to investigate the potential behavior for large number of
164 cycles under a more diverse set of cyclic load levels.

165

166 **ACKNOWLEDGMENTS**

167 The above research was funded by a Theme-based Research Scheme project (T22-502/18-R), a
168 Research Impact Fund project (R5037-18) and two GRF projects (PolyU 15210020, PolyU

169 15210322) from the Research Grants Council of Hong Kong Special Administrative Region
170 Government of China, respectively. The authors of this work also gratefully acknowledged the
171 financial support provided by PolyU (BD8U) and the Research Institute of Land and Space of
172 PolyU (CD82, CD7A).

173 **REFERENCES**

174 Bersan, S., Bergamo, O., Palmieri, L., Schenato, L., & Simonini, P. (2018). Distributed strain
175 measurements in a CFA pile using high spatial resolution fibre optic sensors. *Engineering
176 Structures*, 160, 554-565.

177 Buckley, R. M., Jardine, R. J., Kontoe, S., Parker, D., & Schroeder, F. C. (2018). Ageing and
178 cyclic behaviour of axially loaded piles driven in chalk. *Géotechnique*, 68(2), 146-161.
179 <https://doi.org/10.1680/jgeot.17.P.012>

180 De Battista, N., Kechavarzi, C., Seo, H., Soga, K., & Pennington, S. (2016). Distributed fibre
181 optic sensors for measuring strain and temperature of cast-in-situ concrete test piles.
182 Transforming the Future of Infrastructure through Smarter Information: Proceedings of
183 the International Conference on Smart Infrastructure and ConstructionConstruction, 27–
184 29 June 2016,

185 Iskander, M. G., & Hassan, M. (1998). State of the practice review in FRP composite piling.
186 *Journal of Composites for Construction*, 2(3), 116-120.

187 Iskander, M. G., & Stachula, A. (2002). Wave equation analyses of fiber-reinforced polymer
188 composite piling. *Journal of Composites for Construction*, 6(2), 88-96.

189 Jardine, R., Zhu, B., Foray, P., & Yang, Z. (2013). Interpretation of stress measurements made
190 around closed-ended displacement piles in sand. *Géotechnique*, 63(8), 613-627.

191 Jardine, R. J., & Standing, J. R. (2012). Field axial cyclic loading experiments on piles driven in
192 sand. *Soils and Foundations*, 52(4), 723-736.

193 Ng, C. W., Yau, T. L., Li, J. H., & Tang, W. H. (2001). Side resistance of large diameter bored
194 piles socketed into decomposed rocks. *Journal of Geotechnical and Geoenvironmental
195 Engineering*, 127(8), 642-657.

196 Puech, A. (2013). 'Design for cyclic loading: piles and other foundations'. Proceedings of TC
197 209 workshop,

198 Rimoy, S. P., Jardine, R. J., & Standing, J. R. (2013). Displacement response to axial cycling of
199 piles driven in sand. *Proceedings of the Institution of Civil Engineers-Geotechnical
200 Engineering*, 166(2), 131-146.

201 SharnoubiM.M., E., & NaggarM.H., E. (2012). Axial monotonic and cyclic performance of
202 fibre-reinforced polymer (FRP) – steel fibre-reinforced helical pulldown micropiles
203 (FRP-RHPM). *Canadian Geotechnical Journal*, 49(12), 1378-1392.
204 <https://doi.org/10.1139/cgj-2012-0009>

205 Soga, K. (2014). Understanding the real performance of geotechnical structures using an
206 innovative fibre optic distributed strain measurement technology. *Rivista Italiana di
207 Geotechnica*, 4, 7-48.

208 Sun, Y., Cao, S., Xu, H., & Zhou, X. (2020). Application of distributed fiber optic sensing
209 technique to monitor stability of a geogrid-reinforced model slope. *International Journal
210 of Geosynthetics and Ground Engineering*, 6, 1-11.

211 Tsuha, C. H. C., Foray, P. Y., Jardine, R. J., Yang, Z. X., Silva, M., & Rimoy, S. (2012).
212 Behaviour of displacement piles in sand under cyclic axial loading. *Soils and
213 Foundations*, 52(3), 393-410. <https://doi.org/10.1016/j.sandf.2012.05.002>

214 Zhang, D., Shi, B., Sun, Y., Tong, H., & Wang, G. (2015). Bank slope monitoring with
215 integrated fiber optical sensing technology in Three Gorges Reservoir Area. In
216 *Engineering Geology for Society and Territory-Volume 2* (pp. 135-138). Springer.

217